



Numerical analysis of slide-head-toppling failure

H. Sarfaraz, M.H. Khosravi* and M. Amini

School of Mining Engineering, College of Engineering, University of Tehran, Tehran, Iran

Received 1 June 2019; received in revised form 14 July 2019; accepted 23 July 2019

Keywords

Rock Slopes

Slide-Head-Toppling

Numerical Modeling

Finite Element Method

Abstract

In layered and blocky rock slopes, toppling failure is a common mode of instability that may occur in mining engineering. If this type of slope failure occurs as a consequence of another type of failure, it is referred to as the secondary toppling failure. "Slide-head-toppling" is a type of secondary toppling failures, where the upper part of the slope is toppled as a consequence of a semi-circular sliding failure at the toe of the slope. In this research work, the slide-head-toppling failure is examined through a series of numerical modeling. Phase 2, as a software written based on the finite element method, is used in this work. Different types of slide-head-toppling failures including blocky, block-flexural, and flexural are simulated. A good agreement can be observed when the results of the numerical modeling are compared with those for the pre-existing physical modeling and analytical method.

1. Introduction

In 1968, for the first time, Muler [1] mentioned rotation of natural rock blocks by examining the instabilities overlooking the lake of the Italian Vinot dam. In 1971, Ashby [2] carried out comprehensive studies of single-block toppling and sliding. He was the first to suggest the word "toppling" for this kind of failure. In 1972, Erguvanli and Goodman [3] modeled the toppling failure using a base friction table apparatus. In 1973, De Freitas and Watters [4] presented some examples of this type of failure. Goodman and Bray [5] categorized the toppling failure into two main and secondary types based on the regional observations and physical modeling. For the main types of toppling failures (flexural, blocky, and block-flexural), the governing factor of instability is the weight of the rock mass. However, for the secondary toppling failures, it is stimulated by some external factors. In 1976, Goodman and Barry [6-8] proposed a suitable theory for analysis of the block toppling failure. The solution was presented for several times in a diagram and by a computer code for analyzing the block toppling failure. Apart from the above-mentioned research

works, other studies were conducted with an emphasis on the case studies, physical modeling, theoretical methods, and numerical modeling of block toppling failure, where most of them were based on the classification of Goodman and Berry [9-15]. During 1983 and 1992, Aydan and Kawamoto modeled the toppling failure of the rock slopes using a friction table apparatus [16, 17]. In 1993, Shimizu *et al.* [18] evaluated some examples of flexural toppling failure using the numerical methods based on the finite element and discrete element methods. In 1997, Adhikary *et al.* [19] modeled the flexural toppling failure using a geotechnical centrifuge machine. They conducted a new series of the centrifugal model test during 2007, where the concrete and glass samples with a potential of flexural toppling were used as the modeling materials [20]. Yeung and Wong examined the kinetic conditions in toppling failure using physical modeling and 3D discontinuous deformation analysis (DDA) [21]. Many types of studies were carried out on the numerical simulation of toppling failures using the 2D continuum and discontinuum methods [22-24].

In 2009, Amini *et al.* [25-28] proposed a straightforward solution for toppling failure analysis based on the compatibility principles governing the behavior of cantilever beams. In 2012, Amini *et al.* [29] combined the method of Goodman and Bray with the method of Aydan and Kawamoto in order to introduce a solution for the analysis of the block-flexural toppling failure. In 2017, Guo *et al.* [30] proposed an analytical solution for block toppling failure of rock slopes under dynamic conditions based on the equilibrium method. In 2018, Bowa *et al.* [31] presented an analytical technique for the stability analyses of rock slopes subjected to block toppling failure. In 2019, Liu *et al.* [32] used a 3D discontinuous deformation analysis method for failure mechanisms of toppling rock slopes.

The secondary toppling failure is quite diverse, and various cases have been introduced for these failures. Several papers and reports have been presented for these types of failures [33-41]. One of the common types of secondary toppling failures is slide-head-toppling. In this type of failure, the stratified or blocky rock mass in the upper part of a slope is prone to toppling due to the slide of a soil mass or weathered rock mass in the toe of the slope. The mechanism of this type of failure was initially introduced by Evans [36, 37]. He proposed an analytical approach to assess this kind of instability.

Recently, Amini *et al.* [41] conducted a series of physical models for the slide-head-toppling failure

and developed a theory based on the limit equilibrium. In this work, the physical and theoretical results of Amini *et al.* [41] were examined through numerical simulation, and the results obtained were discussed.

2. Mechanism of slide-head-toppling failure

If a rock slope is formed from two parts with an upper section having a potential of toppling and its toe section with the potential of sliding, then there is a possibility of a slide-head-toppling failure. A schematic representation of this type of slope instability is shown in Figure 1. In addition, a typical open-pit slope with the potential of slide-head-toppling failure in Valencia (Spain) is illustrated in Figure 2 [38].

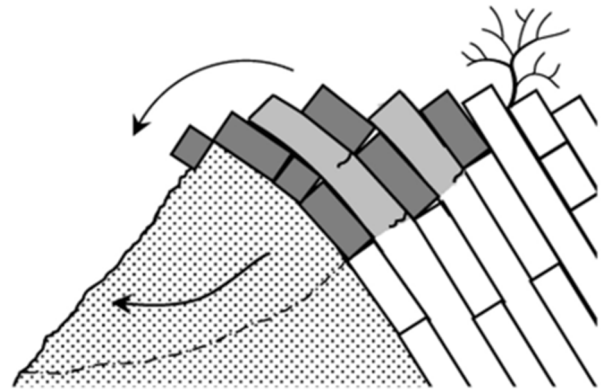


Figure 1. A schematic diagram of the slide-head-toppling failure [41].

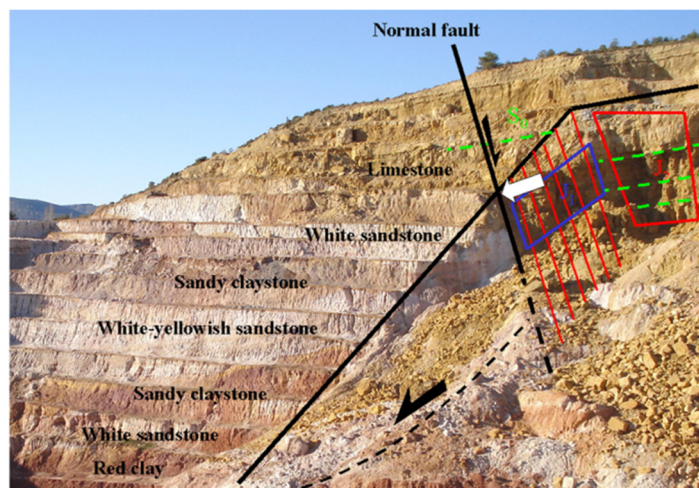


Figure 2. The slope of an open-pit mine with the potential of slide-head-toppling in Spain [38].

In this type of failure, the rock columns in the upper portion of the slope are susceptible to three modes of toppling failures, i.e. blocky, flexural, and block-flexural. As the soil mass in the lower part of the slope has a supportive role for the rock columns, there is a natural interaction between the

soil mass and the rock columns. Therefore, the stability of the rock columns depends on the stability of the soil mass. The physical modeling of Amini *et al.* [38], as a basis of numerical modeling conducted in this research work, is reviewed in the next section.

3. A review of physical modeling

Physical modeling is one of the common procedures used to investigate the mechanism of instability in geomaterials. Amini *et al.* [41] conducted a series of slide-head-toppling physical model tests by means of a tilting table machine shown in Figure 3.

They modeled three modes of secondary toppling, which are illustrated in Figure 4. For the blocky toppling mode, a set of artificial cross-joint was made at the base of blocks so that the overall failure plane inclined at an angle of 20° to the table floor. For the flexural toppling mode, the

continuous blocks were used for modeling; therefore, the blocks were broken at their base due to bending. Finally, in order to model the block-flexural mode, half of the blocks were continuous, while the other half had cross-joints. By tilting of the model, tension cracks appeared at the upper portion of the slope, and the blocks were bent on the soil mass. In the later stages, some horizontal shear displacements appeared on the slope face. Finally, a circular sliding occurred in the soil mass, and the blocks were toppled suddenly [41]. A total number of seven model tests were conducted (Table 1).

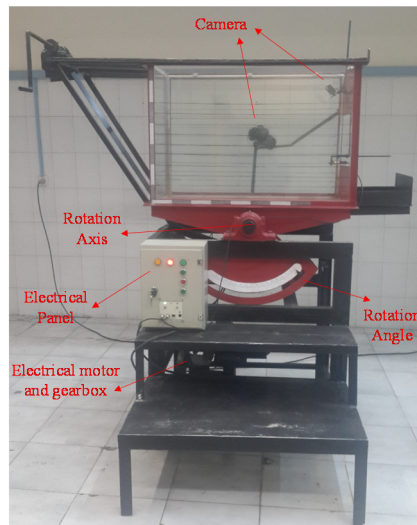


Figure 3. The tilting table apparatus used for physical modeling [41].

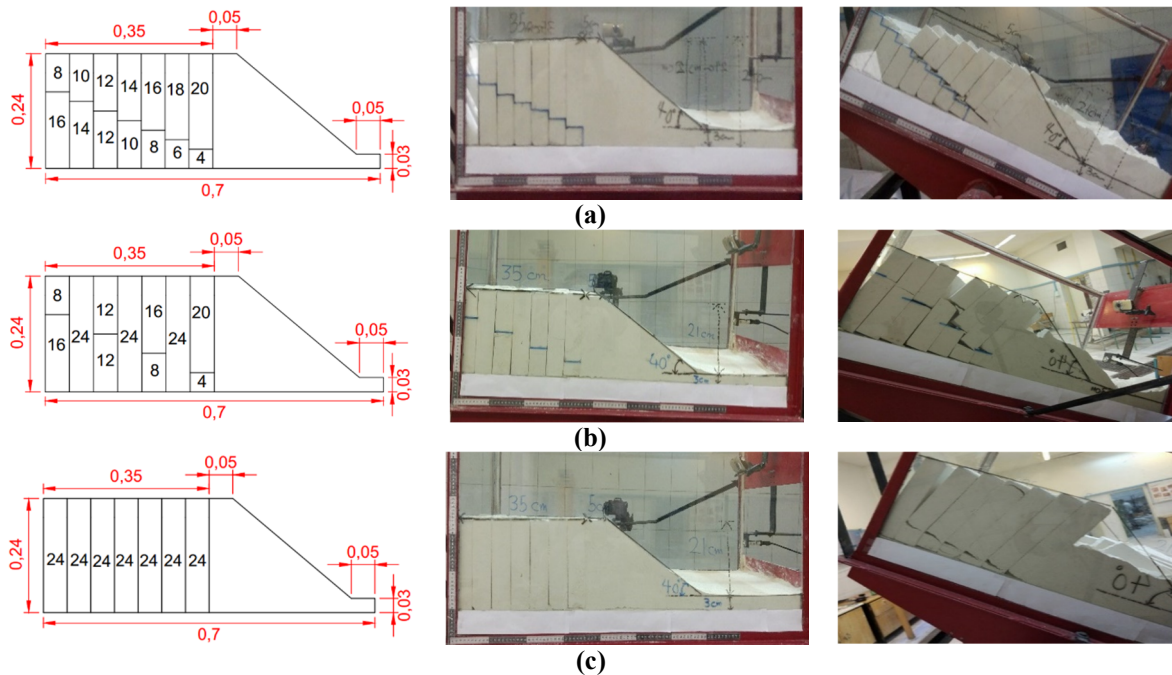


Figure 4. Schematic diagrams and pictures of slide-head-toppling models with a height of 240 mm. (a) block toppling, (b) block-flexural toppling, (c) flexural toppling [41].

Table 1. The slide-head-toppling physical model tests [41].

Model test No.	B20	B24	B30	BF20	BF24	F20	F24
Toppling mode	block	block	block	block-flexural	block-flexural	flexural	flexural
Model height (cm)	20	24	30	20	24	20	24
Table inclination at failure (Degree)	34.5	29	23.5	37	31.5	39	33

4. Numerical modeling

In the recent years, the numerical simulation in rock mechanic problems is widely accepted and is used as a useful tool for the design and stability control of projects. In this work, the results of the physical models were simulated using the numerical software Phase 2. This software, which is based on the finite element method, is a useful tool for the analysis of soil and rock slopes and has been used successfully for an examination of the pure circular and toppling failures. Application and accuracy of the finite element method resulting in the analysis and evaluation of the continuous models have already been confirmed [40]. Therefore, this method can be used to analyze the circular zone of the slide-head-toppling failures. With the addition of joint elements, the introduction of joint elements to the finite element method has enhanced its utility in the analysis of the discontinuing models. In the Phase 2 software, the Goodman joint element is used to evaluate the joints. This element can model the slip of two levels of a joint on each other and their separation. In other words, the joints are analyzed with the help of the Goodman joint element, which allows the model to account for detachment of joint surfaces as well as their sliding over each other. This feature allows the toppling failure to be modeled with this method. Therefore, modeling of the toppling failure is possible in this software.

The Phase 2 software can be used to calculate the stress and displacement during investigation of the slope stability and other issues. The safety factor can be used to check the stability of the slope.

Regarding the shear failure, the safety factor is defined as shown in Equation (1).

$$FOS = \frac{\tau}{\tau_s} \quad (1)$$

where τ and τ_s are the shear strength and shear stress on the slip surface, respectively.

The shear strength is defined according to the Mohr-Coulomb criterion according to Equation (2).

$$\tau = s_0 + \sigma_n \tan \phi \quad (2)$$

where s_0 and σ_n are the cohesion and normal stress on the slip surface, respectively, and ϕ is the friction angle. In this method, the parameters cohesion and friction angle are reduced continuously to the threshold of failure. The stress reduction factor is indicated by SRF. The reduced resistance parameters S_c and ϕ_c are obtained using Equations (3) and (4), respectively.

$$S_c = \frac{S}{SRF} \quad (3)$$

$$\phi_c = \tan^{-1}\left(\frac{\tan \phi}{SRF}\right) \quad (4)$$

For the numerical modeling, the physical and mechanical properties of the materials should be available. The properties of the block and powder are listed in Table 2. Also the properties of the joints between blocks are given in Table 3. The Mohr-Coulomb friction law was used in the numerical modeling. The initial geometry of each model was prepared at the instant of failure in the software. Then the model was analyzed by the shear strength reduction method.

Table 2. Physical and mechanical properties of the materials used in the numerical modeling [41].

Element	Unit weight (kN/m ³)	Modulus of elasticity (MPa)	Poison ratio	Tensile strength (kPa)	Friction angle (peak) (Degree)	Friction angle (residual) (Degree)	Cohesion (peak) (kPa)	Cohesion (residual) (kPa)
Solid block	21.1	10	0.27	14	35	25	100	0
Powder	16	4	0.25	0	28	22.5	0.551	0.35

Table 3. The mechanical properties of joint elements.

Normal stiffness (MPa/m)	Shear stiffness (MPa/m)	Peak cohesion (kPa)	Residual cohesion (kPa)	Peak friction angle (Degree)	Residual friction angle (Degree)
100	1	0	0	32	25

In order to investigate the mechanism of the slide-head-toppling failure, the numerical modeling was investigated based on the type of failure in the upper part of the slope. According to Figure 4, in all numerical models, the boundary conditions are fixed in the table and section of the toe in the two directions x and y, and the blocks are not fixed in any direction and have the freedom of movement (as shown in Figures 5 to 9). The results of the numerical modeling are presented in the following sub-sections.

4.1. Flexural toppling failure

In this type of instability, the solid blocks at the upper part of the slope were completely continuous and could endure tensile stresses. Similar to the physical models, the blocks were broken due to bending. As a result, the soil mass at the toe of the slope slides. The shear strain in the model F24 with a potential of flexural toppling

is shown in Figure 5. According to this figure, the stress reduction factor was calculated at 0.877. Since this type of failure is very sensitive to tensile stresses, the distribution of tensile stresses is shown in Figure 6. This figure illustrates that approximately half of the cross-sections of each block is under the tensile stress.

In the toppling failure, particularly flexural toppling, determining the overall failure plane inside the rock mass is associated with many ambiguities. This plane is frequently located above the plane perpendicular to the dominant discontinuities. The empirical research works have assessed this angle to be between 5 and 15 degrees. In order to confirm the validity of the numerical modeling results, this angle was determined to be 9 degrees for model F24, as illustrated in Figure 7, which is in an acceptable range.

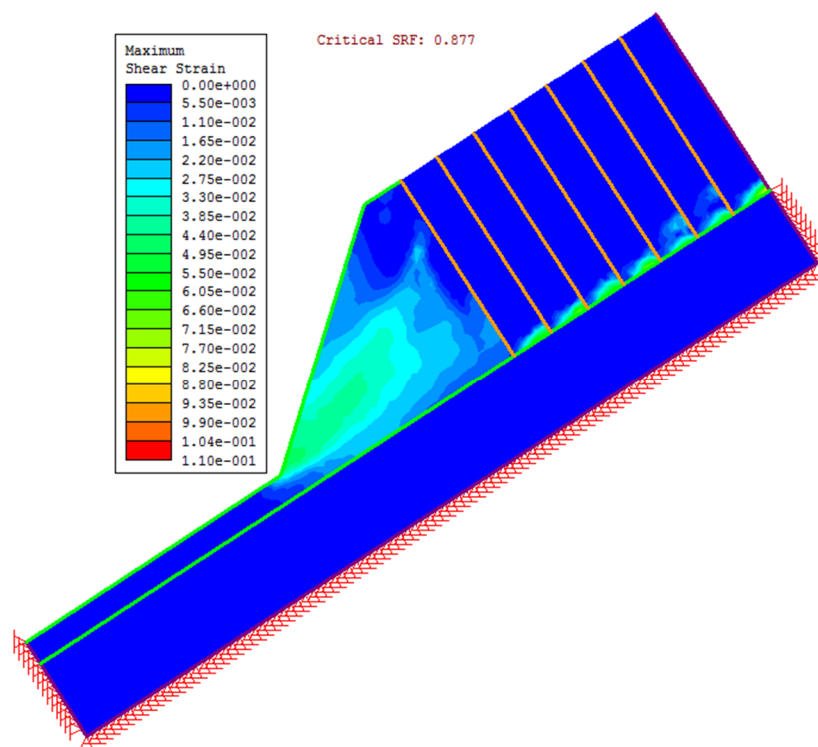


Figure 5. Contours of shear strain in the numerical model F24 (magnification factor of displacements: 1).

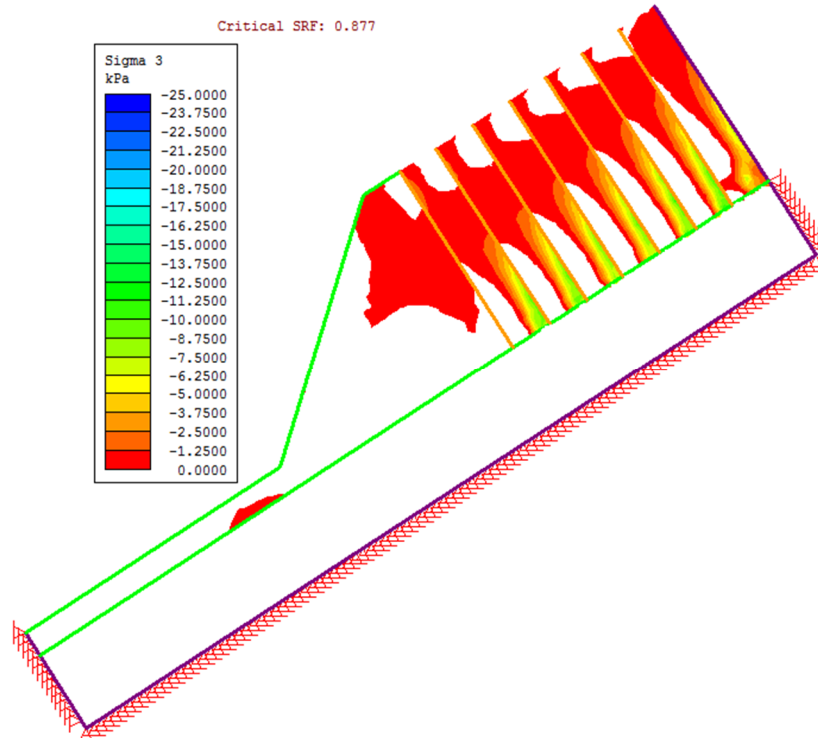


Figure 6. Distribution of tensile stresses in the numerical model F24.

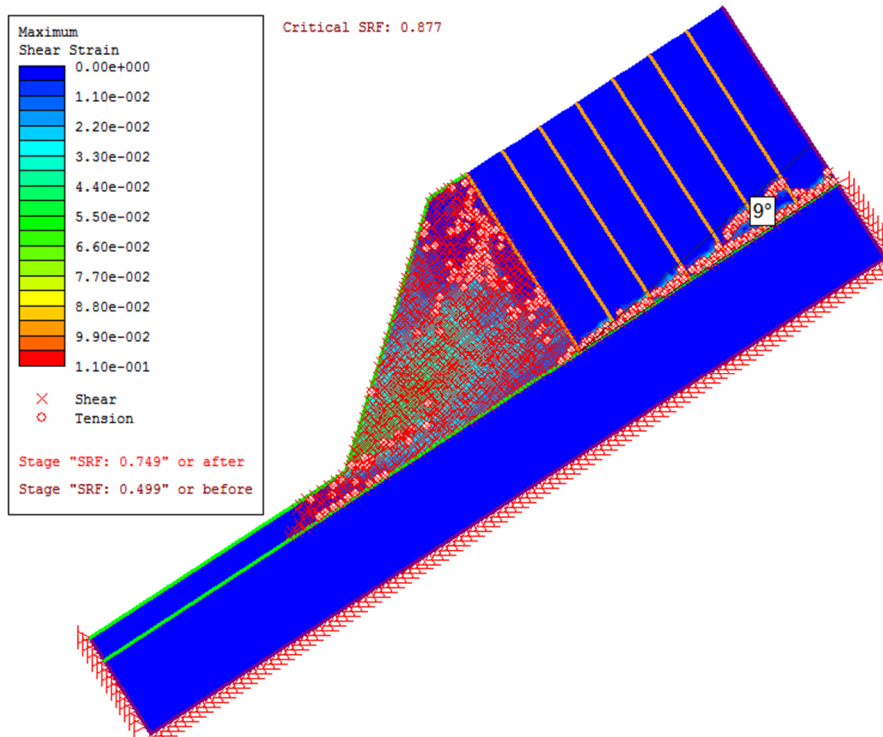


Figure 7. Inclination of the overall failure plane in numerical model F24.

4.2. Block toppling failure

In this kind of instability, due to the presence of cross-joints, the blocks do not tolerate tensile stresses; instead, they topple or slide by loads from upstream blocks. The contours of shear strain in the numerical model B24 are shown in Figure 8, in which the stress reduction factor is

0.894. In this figure, the path of circular failure and the shearing between joints can be observed. Also it can be seen that the blocks have overturned about their base and experienced a pure toppling. In the discussed models, the blocks with the potential of toppling could be separated from those with the sliding potential.

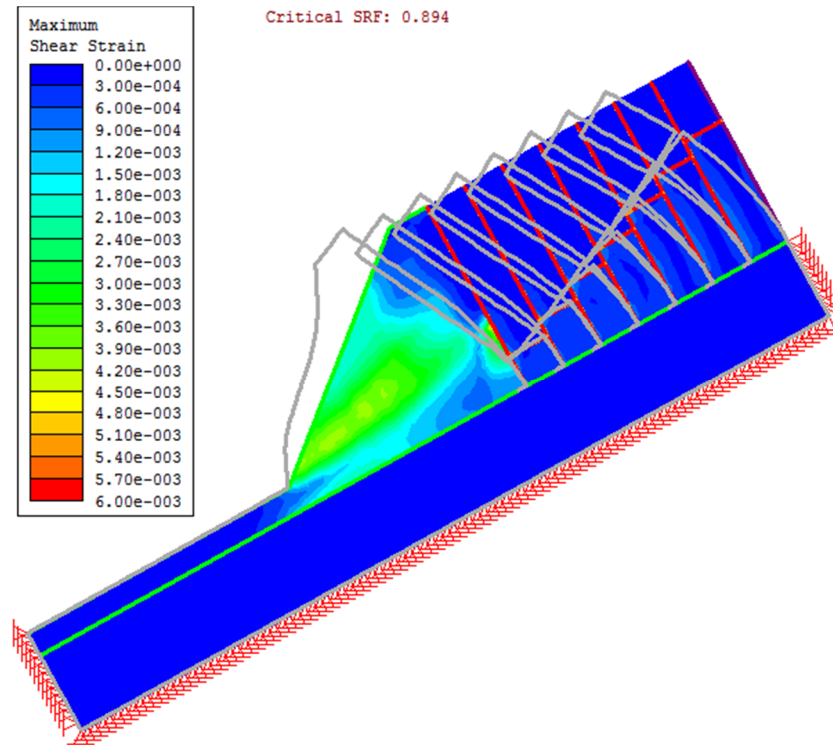


Figure 8. Contours of shear strain in the numerical model B24 (magnification factor of displacements: 100).

4.3. Block-flexural toppling failure

In this instability, due to the pressure included by the weight of the upstream blocks, half of the blocks were broken under the tensile stress (flexural portion), and the other half was separated along the secondary joint (blocky portion), leading to a general toppling failure. The result of

the numerical analysis of model BF24 is presented in Figure 9, where the stress reduction factor is 0.91. The elements and joints yielded under the normal and shear stresses are indicated in this figure. According to this figure, the combination of blocky and flexural toppling is a failure surface that passes through the cross joints.

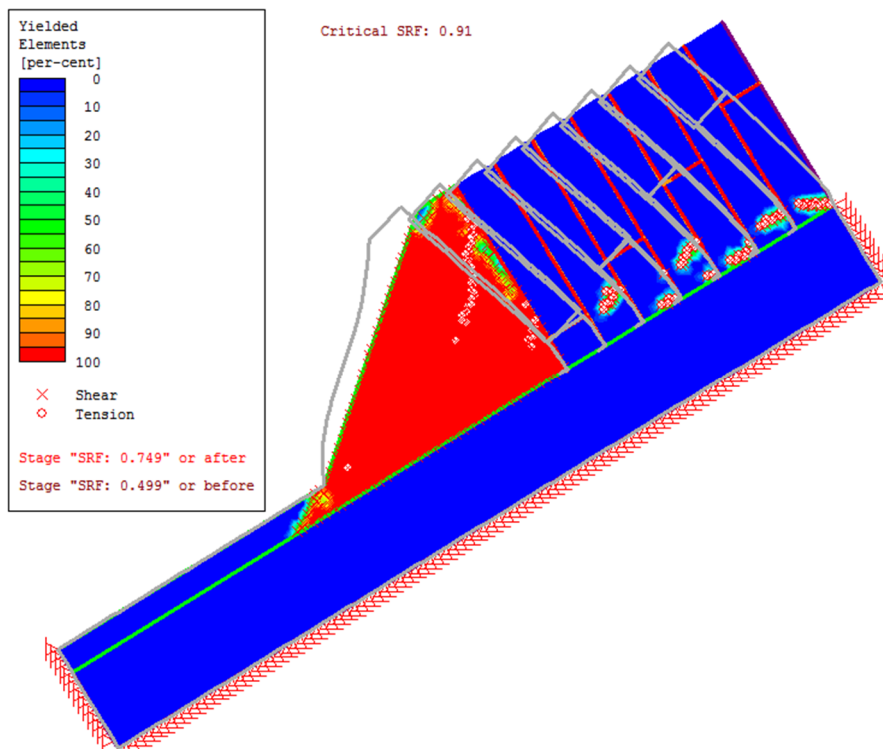


Figure 9. Result of numerical analysis in the model BF24 (magnification factor of displacements: 50).

5. Results and discussions

In this section, the results of the numerical modeling are compared with the corresponding physical modeling to validate the accuracy of the numerical simulation and the Phase 2 software. From the numerical analysis, various diagrams and quantities are extracted, and the results of the physical and numerical modelings are compared. On the other hand, the most suitable quantity for comparison between these models is the critical stress reduction factor. It is possible that in numerical methods this quantity can be assumed

to be equivalent to a safety factor [42]. Since at the moment of failure the safety factor of physical models was equal to one, the critical stress reduction factor of all numerical models should also be equal to one. The safety factor (FS) for the physical model was compared with the stress reduction factor (SRF) of the numerical models in Table 4. The errors between the physical and numerical results are less than 14%, which seems reasonable due to the complicity of the failure mechanism.

Table 4. Comparison of numerical modeling results with the corresponding physical models.

Models	B20	B24	B30	BF20	BF24	F20	F24
FS in physical modeling	1	1	1	1	1	1	1
SRF in numerical modeling	0.86	0.894	0.88	0.935	0.91	0.875	0.877
Error (%)	14	10.6	12	6.5	9	12.5	12.3

Another method used to compare the results of the numerical and physical models is the comparison of the table inclination at the moment of failure. In the numerical models, the line perpendicular to

the rock mass discontinuities coincides with the table inclination. The relative error was calculated using the following relationship and resulted in an average relative error of 10.98%:

$$Relative\ Error = \frac{abs (Table\ Angle_Physical - Table\ Angle_Numerical)}{Table\ Angle_Physical} \tag{5}$$

The maximum table inclination measured in the numerical models was compared with the values predicted by the analytical method developed by Amini *et al.* [41] in Figure 10. This figure shows a good agreement between the numerical and analytical results.

Moreover, the numerical modeling results were compared with both the experimental modeling results and the analytical predictions, illustrated in Figure 11. In all cases, the numerical models estimated the table inclination less than the values measured in the physical models. The analytical

predictions are placed in between the numerical and physical measurements. The underestimation of the numerical models, compared to the physical models, may be related to the shortcomings of FEM codes, such as Phase 2, in the simulation of detachment and displacement along discontinuities. However, it is probably due to the side-effect in the physical modeling as well because the numerical models are assumed two-dimensional with zero side-friction, while there are some side-frictions in the physical models leading to a 3D failure mechanism.

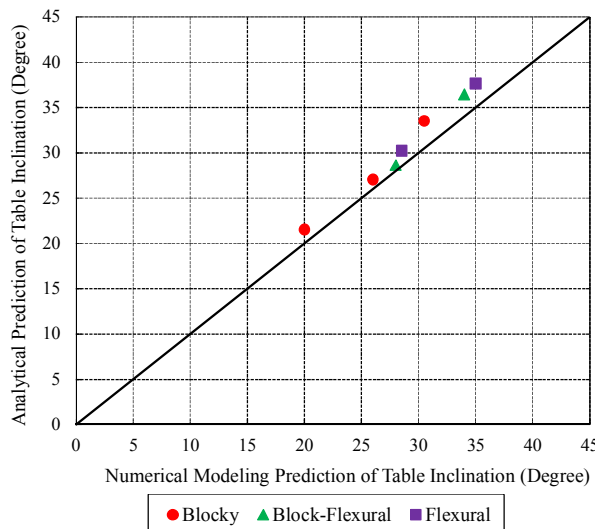


Figure 10. Comparison of the numerical modeling results with analytical predictions.

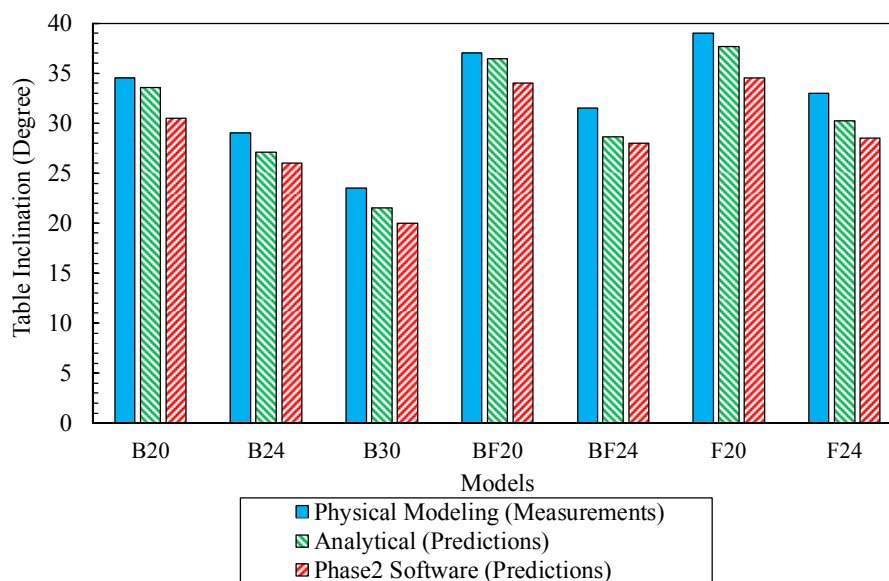


Figure 11. Comparison between the physical, analytical, and numerical results.

6. Conclusions

In this work, the mechanism of the slide-head-toppling failure was investigated through a series of numerical models analyzed in Phase 2 as a finite element software. The results obtained can be concluded as follow:

- In the flexural toppling failure, the rock columns at the upper part of the model slope were bent over the soil mass, broken down due to induced tensile stress, and resulted in a sliding failure at the toe of the slope.
- In the block toppling failure, because of the presence of secondary joints, the blocks did not withstand tensile stresses. The blocks were topped or slide due to the upstream loads, and finally, led to a sliding failure at the toe of the slope.
- In the blocky-flexural toppling failure, half of the blocks were broken down under the tensile stress, and the other half was separated along the secondary joints. However, all the blocks were toppled with each other, leading to a sliding failure at the toe of the slope.
- Comparison of the numerical and physical modelings illustrated an underestimation of up to 14% for the safety factor in numerical models. This is due to the plane strain assumption in the numerical analysis, while the side-friction in the physical models violated this assumption.
- Comparison of the numerical modeling and analytical predictions presented a maximum error of 9%, which is acceptable due to the complexity of the failure mechanism in slide-head-toppling. The results of this research work indicated that the finite element method could be used accurately for evaluating the

stability analysis of slopes with a potential of slide-head-toppling failure.

- The use of distinct element codes such as UDEC and PFC software for simulation of this failure is suggested for future studies.

References

- [1]. Mueller, L. (1968). New considerations on the Vaiont slide. *Rock Mechanics & Engineering Geology*.
- [2]. Ashby, J. (1971). Sliding and toppling modes of failure in models and jointed rock slopes, Imperial College, University of London.
- [3]. Erguvanli, R. and Goodman. K. (1970). Applications of models to engineering geology for rock excavations, *Assoc Eng Geol*, 9 P.
- [4]. de Freitas, M.H. and Watters, R.J. (2009). Discussion: Some field examples of toppling failure, *Géotechnique*. 24 (4): 691-693.
- [5]. Wyllie, D.C., Mah, C.W. and Hoek, E. (2004). *Rock slope engineering : civil and mining*. Spon Press.
- [6]. Choquet, D.D.B. and Tanon, P. (1985). Nomograms for the assessment of toppling failure in rock slopes, in 26th US Symposium on Rock Mechanics. pp. 19-30.
- [7]. Turner, R.L. and Schuster, A. (1996). *Landslides investigation and mitigation*. Transportation Research Board, Washington.
- [8]. Tatone, B.S.A. and Grasselli, G. (2010). ROCKTOPPLE: A spreadsheet-based program for probabilistic block-toppling analysis, *Comput. Geosci*. 36 (1): 98-114.
- [9]. Savigny, M.A.P.K.W. (1990). Numerical modelling of toppling, *Can. Geotech. J.* 4: 823-834.
- [10]. Cruden, D.M. (1989). Limits to common

- toppling. *Can. Geotech. J.* 26 (4): 737-742.
- [11]. Bobet, A. (2002). Analytical solutions for toppling failure, *Int. J. Rock Mech. Min. Sci.* 36 (7): 971-980.
- [12]. Sagaseta, C., Sánchez, J.M. and Cañizal, J. (2001). A general analytical solution for the required anchor force in rock slopes with toppling failure, *Int. J. Rock Mech. Min. Sci.* 38 (3): 421-435.
- [13]. Brideau, M.A. and Stead, D. (2010). Controls on block toppling using a three-dimensional distinct element approach, *Rock Mech. Rock Eng.* 3 (3): 241-260.
- [14]. Babiker, A.F.A., Smith, C.C., Gilbert, M. and Ashby, J.P. (2014). Non-associative limit analysis of the toppling-sliding failure of rock slopes, *Int. J. Rock Mech. Min. Sci.* 71: 1-11.
- [15]. Alejano, L.R., Carranza-Torres, C., Giani, G.P. and Arzúa, J. (2015). Study of the stability against toppling of rock blocks with rounded edges based on analytical and experimental approaches, *Eng. Geol.* 195: 172-184.
- [16]. Aydan, O. and Kawamoto, T. (1992). The stability of slopes and underground openings against flexural toppling and their stabilisation, *Rock Mech. Rock Eng.* 3 (3): 143-165.
- [17]. Aydan, T. and Kawamoto, Ö. (1987). Toppling failure of discontinuous rock slopes and their stabilization (in Japanese), *J. Japan Min. Soc.* 103: 673-770.
- [18]. Shimizu, T., Aydan, Y. and Kawamoto, Ö. (1993). Several toppling failures in Japan and their back analysis, in *Assessment and Prevention of Failure Phenomena in Rock Engineering Conference*. pp. 879-885.
- [19]. Adhikary, D.P., Dyskin, A.V., Jewell, R.J. and Stewart, D.P. (1997). A study of the mechanism of flexural toppling failure of rock slopes, *Rock Mech. Rock Eng.* 30 (2): 75-93.
- [20]. Adhikary, D.P. and Dyskin, A.V. (2007). Modelling of progressive and instantaneous failures of foliated rock slopes, *Rock Mech. Rock Eng.* 40 (4): 349-362.
- [21]. Yeung, M.R. and Wong, K.L. (2007). Three-dimensional kinematic conditions for toppling, *Proc. 1st Canada-US Rock Mech. Symp. - Rock Mech. Meet. Soc. Challenges Demands*. 1: 335-339.
- [22]. Cundall, P.A. (1971). A computer model for simulating progressive large-scale movements in blocky rock systems, in *Proceedings of the Symposium of the International Society of Rock Mechanics*, Nancy 2, 8: 2.
- [23]. Pritchard, M.A. and Savigny, K.W. (1991). The Heather Hill landslide: an example of a large scale toppling failure in a natural slope, *Can. Geotech. J.* 28: 410-422.
- [24]. Alzo'ubi, A.K., Martin, C.D. and Cruden, D.M. (2010). Influence of tensile strength on toppling failure in centrifuge tests, *Int. J. Rock Mech. Min. Sci.* 47 (6): 974-982.
- [25]. Amini, M. (2009). *Dynamic and static slope stability analysis and stabilization of flexural toppling failure (Theoretically, experimentally and case histories)*, Tehran, Iran.
- [26]. Majdi, A. and Amini, M. (2011). Analysis of geo-structural defects in flexural toppling failure, *Int. J. Rock Mech. Min. Sci.* 45 (2): 175-186.
- [27]. Aydan, M. and Amini, Ö. (2009). An experimental study on rock slopes against flexural toppling failure under dynamic loading and some theoretical considerations for its stability assessments, *J. Sch. Mar. Sci. Technol.* 7: 25-40.
- [28]. Amini, M., Majdi, A. and Aydan, Ö. (2009). Stability analysis and the stabilisation of flexural toppling failure, *Rock Mech. Rock Eng.* 42 (5): 751-782.
- [29]. Amini, M., Majdi, A. and Veshadi, M.A. (2012). Stability analysis of rock slopes against block-flexure toppling failure, *Rock Mech. Rock Eng.* 45 (4): 519-532.
- [30]. Guo, S., Qi, S., Yang, G., Zhang, S. and Saroglou, C. (2017). An Analytical Solution for Block Toppling Failure of Rock Slopes during an Earthquake, *Appl. Sci.* 7 (10): 108-116.
- [31]. Bowa, V.M., Xia, Y. and Kabwe, E. (2018). Analytical technique for stability analyses of rock slopes subjected to block toppling failure, *Min. Technol.* pp. 1-11.
- [32]. Liu, G., Li, J. and Kang, F. (2019). Failure Mechanisms of Toppling Rock Slopes Using a Three-Dimensional Discontinuous Deformation Analysis Method, *Rock Mech. Rock Eng.* pp. 1-24.
- [33]. Mohtarami, E., Jafari, A. and Amini, M. (2014). Stability analysis of slopes against combined circular-toppling failure, *Int. J. Rock Mech. Min. Sci.* 67:43-56.
- [34]. Tsesarsky, M. and Hatzor, Y.H. (2009). Kinematics of overhanging slopes in discontinuous rock, *J. Geotech. Geoenvironmental Eng.* 135 (8): 1122-1129.
- [35]. Frayssines, M. and Hantz, D. (2009). Modelling and back-analysing failures in steep limestone cliffs, *Int. J. Rock Mech. Min. Sci.* 46 (7): 1115-1123.
- [36]. Evans, R.S. (1981). An analysis of secondary toppling rock failures the stress redistribution method, *Q. J. Eng. Geol. Hydrogeol.* 14 (2): 77-86.
- [37]. Nichol, S.L., Hungr, O. and Evans, S.G. (2002). Large-scale brittle and ductile toppling of rock slopes, *Can. Geotech. J.* 39 (4): 773-788.

[38]. Alejano, L.R., Gómez-Márquez, I. and Martínez-Alegria, R. (2010). Analysis of a complex toppling-circular slope failure, *Eng. Geol.* 114 (1): 93-104.

[39]. Amini, M., Ardestani, A. and Khosravi, M.H. (2017). Stability analysis of slide-toe-toppling failure, *Eng. Geol.* 228: 82-96.

[40]. Amini, M. and Ardestani, A. (2019) Stability analysis of the north-eastern slope of Daralou copper open pit mine against a secondary toppling failure,

Eng. Geol. 249: 89-101.

[41]. Amini, M., Sarfaraz, H. and Esmacili, K. (2018). Stability analysis of slopes with a potential of slide-head-toppling failure, *Int. J. Rock Mech. Min. Sci.* 112: 108-121.

[42]. Zienkiewicz, O.C., Humpheson, C. and Lewis, R.W. (1975). Associated and non-associated viscoplasticity and plasticity in soil mechanics. *Geotechnique.* 25 (4): 671-689.

مدل‌سازی عددی شکست لغزش-واژگونی در رأس

حسن سرفراز، محمد حسین خسروی* و مهدی امینی

دانشکده مهندسی معدن، دانشکده فنی، دانشگاه تهران، ایران

ارسال ۲۰۱۹/۶/۱، پذیرش ۲۰۱۹/۷/۲۳

* نویسنده مسئول مکاتبات: mh.khosravi@ut.ac.ir

چکیده:

شکست واژگونی یکی از ناپایداری‌های رایج در شیروانی‌های سنگی می‌باشد. اگر این نوع گسیختگی به دنبال گسیختگی دیگری رخ دهد، شکست واژگونی ثانویه اطلاق می‌شود. شکست لغزش-واژگونی در رأس، یکی از مهم‌ترین انواع شکست واژگونی ثانویه است که بخش فوقانی شیروانی واژگون شده و فشار ناشی از واژگونی بلوک‌های سنگی در تاج شیروانی منجر به لغزش توده خاک در پاشنه شیروانی می‌شود. در این پژوهش، شکست لغزش-واژگونی در رأس، از طریق یک سری مدل‌سازی عددی مورد ارزیابی قرار گرفته است. نرم‌افزار Phase 2 بر مبنای روش عددی المان محدود در این پژوهش استفاده شده است. انواع مختلفی از شکست لغزش-واژگونی در رأس شامل شکست بلوکی، بلوکی-خمشی و خمشی مدل‌سازی شده‌اند. نتایج مدل‌سازی عددی با مدل‌های فیزیکی موجود و روش تحلیلی مقایسه شد. مقایسه این نتایج نشان داد که بین نتایج مدل‌سازی عددی با مدل‌های فیزیکی و روش تحلیلی تطابق قابل قبولی وجود دارد.

کلمات کلیدی: شیروانی سنگی، لغزش-واژگونی در رأس، مدل‌سازی عددی، روش المان محدود.